

EXPLORATIONS IN COMMUNICATION SYSTEMS USING A VIRTUAL TOOLKIT

Murat Tanyel
Dordt College

Abstract

A typical communication systems course is rich with processes that are best described by block diagrams. While a typical textbook on the subject may provide examples on the applications of these processes, students are motivated when these block diagrams come alive as they implement these processes and are able to test signals at each block. Such an endeavor requires hardware, space and time allocations that not every institution is prepared to commit. The next best teaching tools are computer simulations in which students can observe signals at each stage of the process. Preparation of such simulations is simplified by software development tools tailored for digital signal processing, such as MATLAB, which has become the standard package most recent communication systems books have adopted. Recent development of data-driven graphical programming languages has provided an improvement over textual languages such as MATLAB by enhancing the conceptual link from the block diagrams of these processes to their computer simulations. This paper is a follow-up on last year's presentation¹, which discussed the development of a virtual toolkit in LabVIEW. It will report on the use of the toolkit in a three-credit *Communication Systems* course, with examples of how this toolkit was used as an exploratory tool to probe further into the simulated systems.

I. Introduction

This paper is a follow-up on a recent paper that describes a simulation toolkit for communication systems and its development with a freshman as the programmer¹. In that paper we stated that in the absence of hardware that would reinforce the theoretical presentation, computer simulations of the systems described in class are the next available tools to bring these concepts alive. We also described the particular class environment and the process in which the software development tool, namely LabVIEW, was chosen. Although MATLAB is the standard software tool employed in the areas of signals and systems, as evidenced by the proliferation of books²⁻⁴ devoted to MATLAB based exercises in those subjects, the choice of the software tool is justified in ^{1, 5, 6}. In a separate paper, Adams and I discuss this choice from an engineering design aesthetics point of view⁷.

This paper will report on the first-time use of the toolkit in EGR 363, *Communication Systems* course offered at Dordt College in Spring 2002. Section II will provide an overview of the in-class presentations that made use of the toolkit while Section III will review some examples that reveal the exploratory facet of the toolkit. Section IV will discuss the student projects and will

offer a sample. I will then conclude with a discussion on the present state of the toolkit and on possible future developments.

II. Presentations with the Toolkit

Communication Systems classes and other upper level electrical engineering classes with low enrollments are held in small classrooms that do not have built-in computer and projection systems. For such classrooms, the engineering department has a *COW* (*computer on wheels*, a very appropriate acronym for a college in a rural setting), a personal computer with a projection system on a cart that may be wheeled around. This mobile PC has a network card and may be connected to the college-wide network through network connectors that are located in every classroom. The LabVIEW software development system is installed on the engineering COW. So any *virtual instrument* (or *VI*, a term used for LabVIEW programs) that I develop and save on the network drive may be easily run in any classroom. I use the COW in most *Communication Systems* classes to demonstrate the concepts covered on that day's topic.

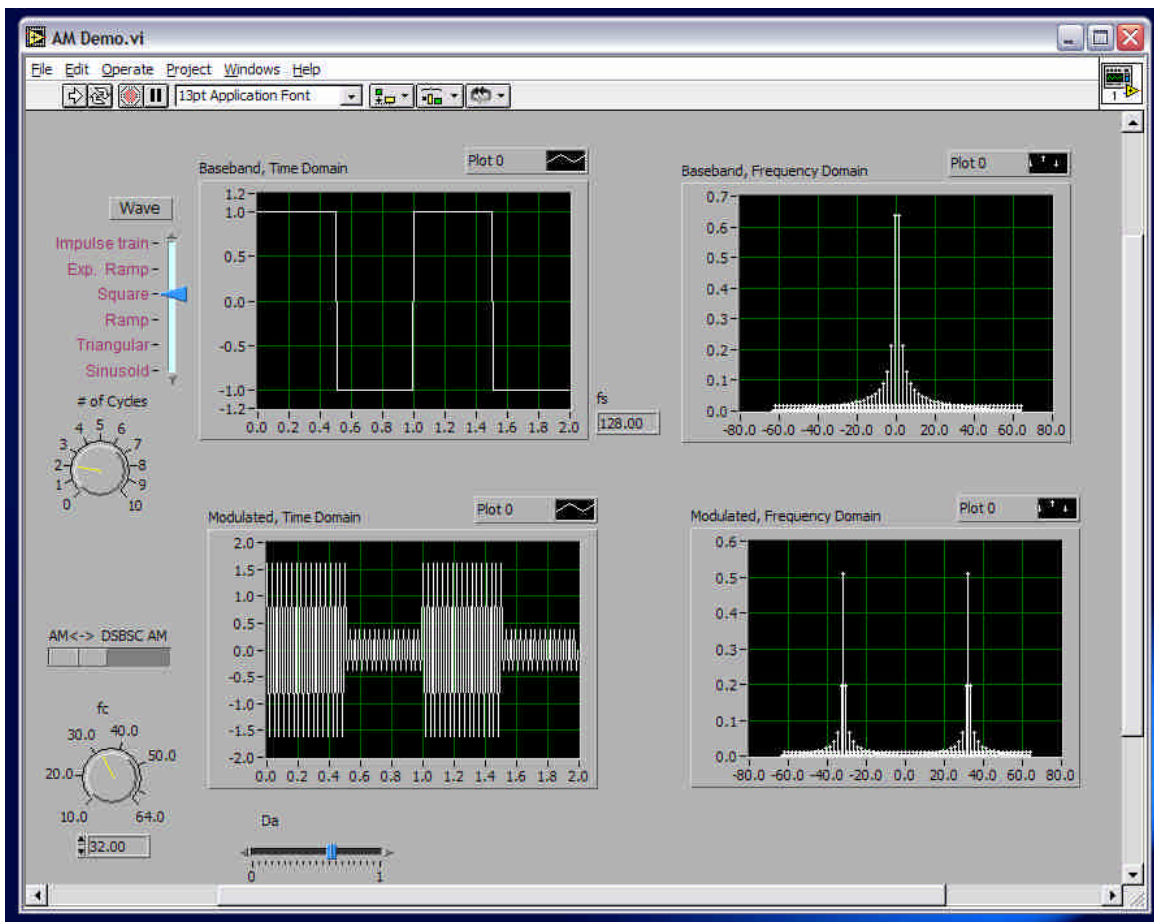


Figure 1: Demonstration of Amplitude Modulation (AM) using the toolkit.

Fig. 1 depicts the front panel of a VI that I use to demonstrate Amplitude Modulation (AM). The effectiveness of this VI is amplified when it is run in continuous mode, in which the VI runs, monitoring its inputs and adjusting its outputs, repeatedly until the stop button is pressed. In this mode, it becomes very easy to change parameters and see the results immediately. For this particular demonstration, one can easily switch through the different kinds of periodic signals as the baseband signal (upper left sliding switch in Fig. 1) and can observe how the modulated signal looks both in time and frequency domain. The frequency of the carrier signal (lower left knob) may be varied and the students watch as the replica of the baseband spectrum moves up and down the frequency band in the lower right graph. It is this continuous mode of operation that makes in-class demonstrations attractive. The ability to change parameters and obtain immediate results is a definite enhancement over standard and static textbook examples.

The above example is one of the many demos I use. Other demos in the same spirit, showing PAM, FM and PM and their spectra have been useful in class.

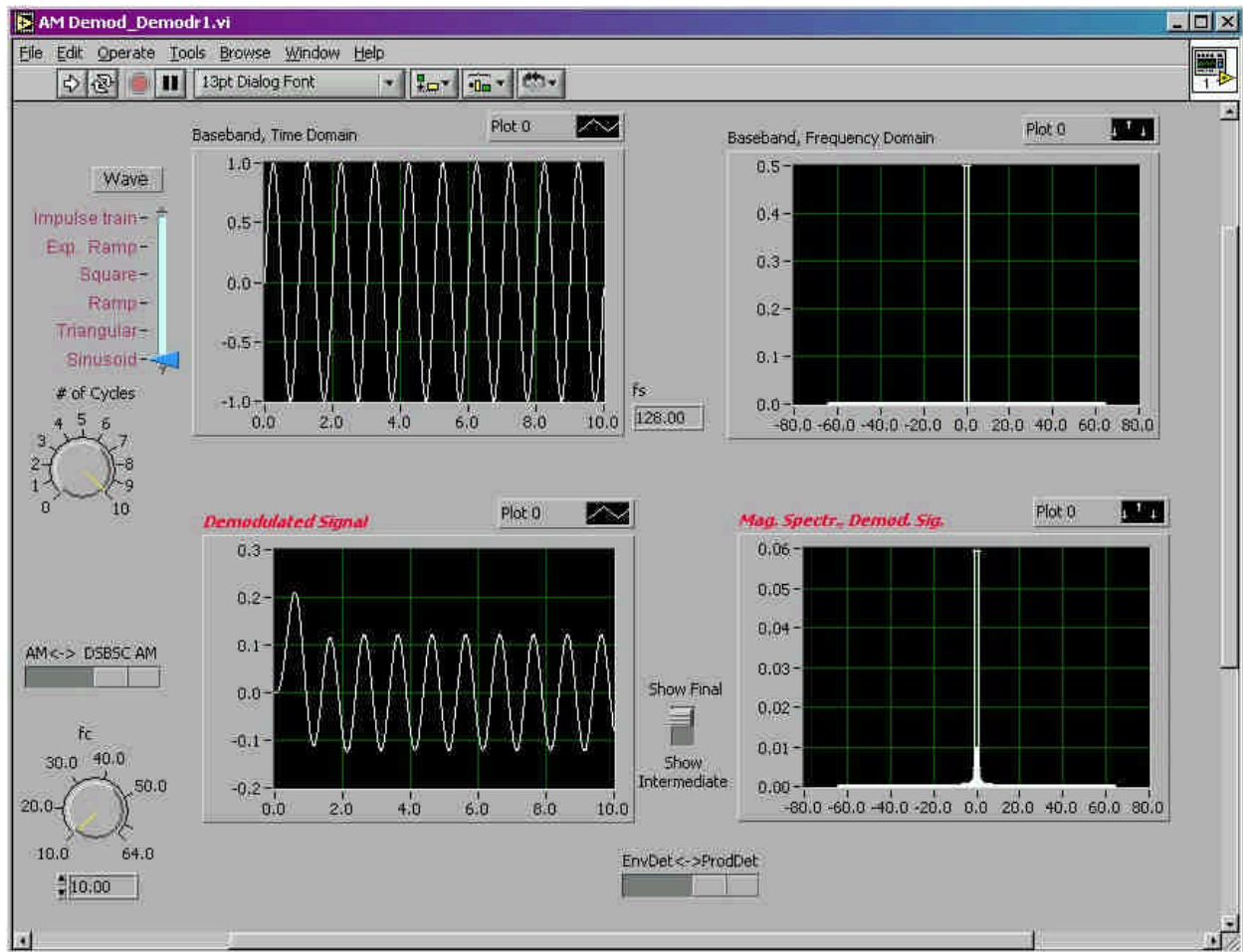


Figure 2: The VI to demonstrate AM demodulation in action.

III. Exploratory Demonstrations

Fig. 2 displays the front panel of the VI that I use to demonstrate the detection of AM signals. With this VI, one can select the type of the baseband signal with the selector in the upper left (labeled “Wave” in Fig. 2) from a number of periodic waveforms and specify the number of cycles to be generated. The fundamental frequency of this waveform is 1 Hz. The baseband signal and its magnitude spectrum are displayed in the upper graphs of the VI. This signal is modulated by a carrier whose frequency may be specified by the knob in the lower left corner of the VI’s panel. The switch toward the middle of the left hand-side of the panel (labeled “AM <- > DSBSC AM”) chooses the type of modulation. If the switch is to the left, AM is employed, which may be expressed by the equation:

$$s(t) = A_c[1 + D_a m(t)]\cos w_c t \quad (1)$$

where $s(t)$ is the modulated signal, A_c is the amplitude of the carrier (assumed to be 1 in this VI), D_a is the modulation index, $m(t)$ is the baseband (message) signal and $w_c (= 2\pi f_c)$ is the carrier frequency. If the same switch is to the right, the *double-sideband suppressed carrier* (DSB-SC) AM is employed, expressed by:

$$s(t) = A_c m(t) \cos w_c t \quad (2).$$

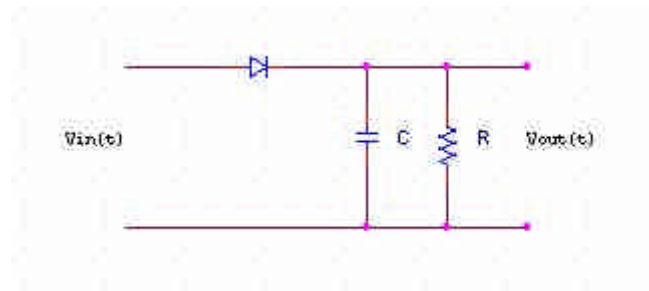


Figure 3: *Envelope detector.*

AM signals may be demodulated by an *envelope detector* comprised of a diode and a lowpass RC filter (Fig. 3) whereas DSB-SC AM signals require a product detector which involves multiplying the signal with a replica of the carrier again:

$$v_{\text{int}}(t) = s(t) \cdot A_0 \cos(w_c t + q_0) = A_c m(t) \cos w_c t \cdot A_0 \cos(w_c t + q_0) \quad (3)$$

This operation separates the signal into a low frequency component, centered around DC, and a high frequency component, centered around $2w_c$:

$$v_{\text{int}}(t) = \frac{1}{2} A_c A_0 m(t) \cos q_0 + \frac{1}{2} A_c A_0 m(t) \cos(2\omega_c t + q_0) \quad (4)$$

Low-pass filtering $v_{\text{int}}(t)$ of eq. 3 or 4 will recover a replica of the original baseband signal:

$$\hat{m}(t) = \frac{1}{2} A_c A_0 m(t) \cos q_0 = Km(t) \quad (5).$$

The lower two graphs of Fig. 2 display the recovered message signal and its magnitude spectrum. I should note that the low-pass filter used introduces some transients, which may be observed in the time-domain representation of the demodulated signal and, due to the record length, these transients contribute a visible difference between the shapes of the magnitude spectrum of $m(t)$ and $\hat{m}(t)$. The intermediate signal (of eq. 4) of the product detector can be easily derived mathematically, either using trigonometric identities as I have done in going from eq. 3 to eq. 4 or using the property that multiplication in time domain results in a convolution in frequency domain. In either case, the resulting spectrum is a replica of the message spectrum around DC and another translated to $2f_c$. Fig. 4 is a snapshot from the front panel of the VI in Fig. 2 displaying the intermediate signal (before low-pass filtering) of the product detector. In this case, a carrier signal of 10 Hz is used to modulate a sinusoidal message of 1 Hz. We can see, in Fig. 4 (graph labeled “Mag. Spectr., Inter. Sig.”), that the 1 Hz message is replicated around the origin as well as around 20 Hz. There is no spectral component at 20 Hz (or at DC) because the method employed is double sideband *suppressed carrier*.

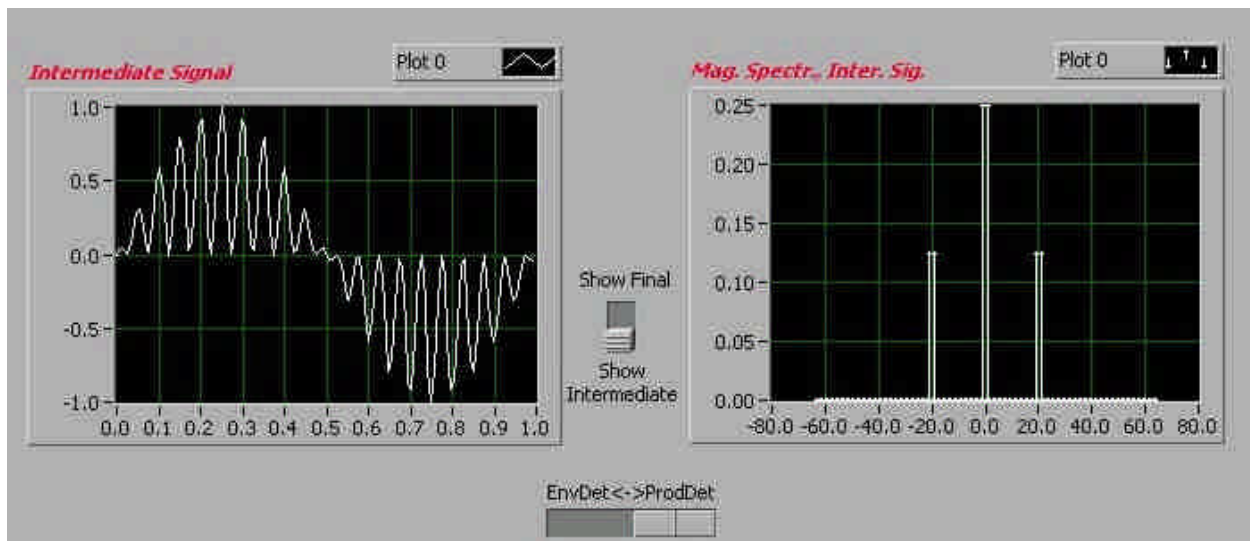


Figure 4: The intermediate signal $[v_{\text{int}}(t)$ of eq. 4] from a product detector. The left graph displays the time domain signal and the right graph displays its magnitude spectrum.

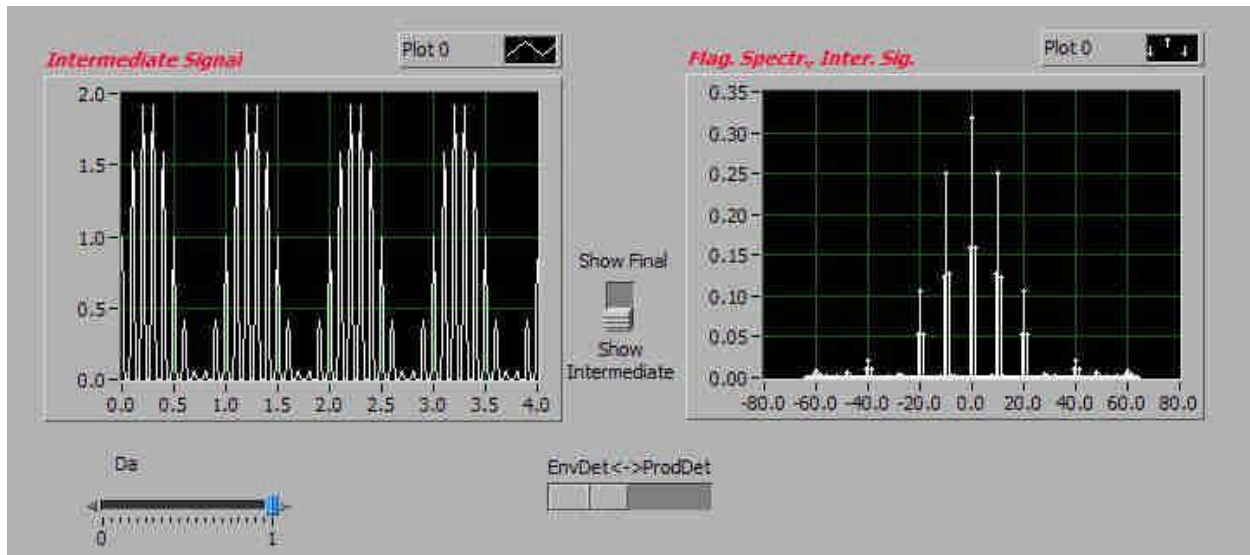


Figure 5: The intermediate signal, that is, the signal that would be obtained without low-pass filtering from an envelope detector.

The mathematical development for the product detector is well understood and derivations like that of equations 3-5 may be found in most textbooks on communication systems, including the textbook chosen for this course⁸. The envelope detector, on the other hand, involves a diode which is a nonlinear device. Since most undergraduate students have been exposed to primarily linear system theory, the nonlinear device in the envelope detector presents a challenge to the mathematical analysis of this method. A cursory scan through introductory textbooks on the subjects reveals a gap in the analysis of the envelope detector. So, a display of the magnitude spectrum of the intermediate signal (the signal that would be obtained if the RC lowpass filter of Fig. 3 were absent) is an exploration for my students, the result of which they could not find in their textbook. Fig. 5 displays the time domain signal and its magnitude spectrum for the envelope detector applied on an AM signal with the following parameters (of eq. 1): $f_c = 10$ Hz, $D_a = 1$ and $m(t)$ is a sinusoidal of 1 Hz. A comparison of the magnitude spectra of the intermediate signals of the product detector (Fig. 4) and the envelope detector (Fig. 5) reveals that both signals contain a replica of the message around DC, which constitutes the received message when low-pass filtered. The signal of Fig. 5 has a DC component because the carrier is not suppressed in regular AM. The intermediate signal of the product detector has a replica around $2f_c$ as predicted, but that of the envelope detector has replicas around f_c , $2f_c$, $4f_c$ and $6f_c$. Where do all these spectral components come from? This is an exercise that an inquisitive student may be encouraged to probe further. Since the simulation uses the model of an ideal diode in the envelope detector, an explanation with linear system theory is possible. The action of the diode may be modeled with the multiplication of the modulated signal with a pulse train of 50 % duty cycle at the same frequency (and phase) as the carrier signal. This is plotted in Fig. 6 for our example, where the carrier is a 10 Hz sinusoidal wave.



Figure 6: A pulse train of 50 % duty cycle at 10 Hz.

Since the model involves multiplication in time domain, the spectrum of the resulting signal will be the spectrum of the modulated signal convolved with the spectrum of the pulse train. In the “Signals and Spectra” chapter of the textbook⁸, the spectrum of a pulse train with 50 % duty cycle is found to be:

$$|W(f)| = \sum_{n=-\infty}^{\infty} \frac{A}{2} \left| \frac{\sin\left(\frac{np}{2}\right)}{\frac{np}{2}} \right| \delta(f - nf_0) \quad (6)$$

where $W(f)$ is the spectrum of the pulse train, A is its amplitude, f_0 is its frequency and $\delta(\cdot)$ is the Dirac delta (impulse) function. The spectrum of a 10 Hz pulse train of amplitude 1 is plotted in Fig. 7. The dashed lines in Fig. 7 trace the envelope (which is a *sinc* pattern) and the solid lines represent the impulses that make up the magnitude spectrum. The spectrum is made up of impulses at DC, at $\pm f_0$, and at odd harmonics, following an envelope $[E(f)]$ of

$$E(f) = \frac{1}{2} \left| \frac{\sin\left(\frac{pf}{20}\right)}{\frac{pf}{20}} \right| \quad (7).$$

To obtain the intermediate signal spectrum, one would convolve the spectrum of Fig. 7 with that of the spectrum of the modulated signal depicted in Fig. 8. A summary of the convolution of the two spectra is as follows: The DC component of $W(f)$ (Fig. 7) convolved with $S(f)$ (Fig. 8) gives rise to the spectral components around ± 10 Hz of the spectrum in Fig. 5. The convolution of the ± 10 Hz components of $W(f)$ with $S(f)$ will give rise to the spectral components around DC and contribute to the spectral components around ± 20 Hz in Fig. 5. The convolution of the ± 30 Hz components of $W(f)$ with $S(f)$ will contribute to the spectral components around ± 40 Hz and to those around ± 20 Hz while the convolution of the ± 50 Hz components of $W(f)$ with $S(f)$ will contribute to the spectral components around ± 60 Hz and to those around ± 40 Hz. This

explanation is enough to explain the predominant peaks around DC, $\pm f_c$, $\pm 2f_c$, $\pm 4f_c$ and $\pm 6f_c$ of Fig. 5. The components beyond these frequencies can be accounted for by taking into consideration the aliasing that also occurs due to the discrete nature of the simulation.

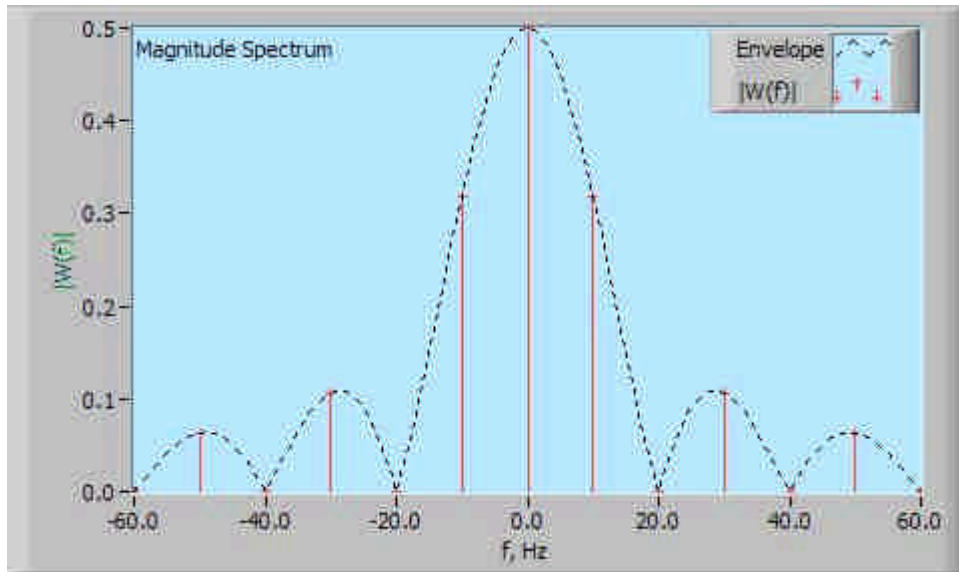


Figure 7: Magnitude spectrum of a 10 Hz, 50% duty cycle pulse train.

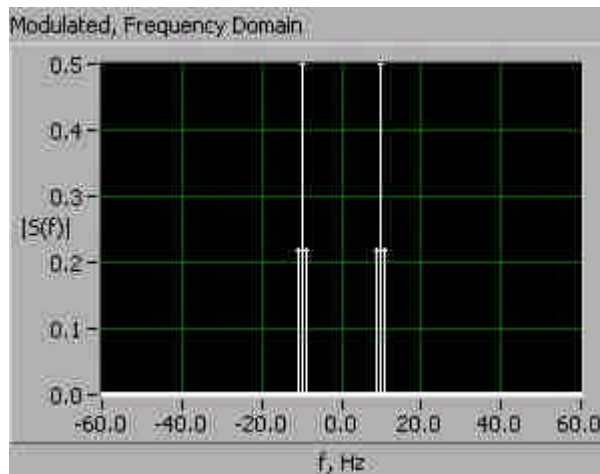


Figure 8: Spectrum of a 1 Hz sinusoid amplitude modulated by a 10 Hz carrier wave.

IV. Student Projects

This year, students in the communications class were asked to develop some new simulations in addition to the ones they had worked with in class. There were six students in class and they formed teams of two, each working on a topic they were interested in. One group worked on companding, another worked on pulse coded modulation (PCM) while the third worked on M-

ary Phase-Shift Keying (MPSK). MPSK is a method of transmitting digital information over analog lines. The binary information is first converted into a multilevel signal (of M levels) and this multilevel signal determines the discrete phase angles of the complex envelope of the MPSK signal. A plot of the permitted values of the complex envelope is called a *signal constellation*. Fig. 9 is a snapshot from the front panel of the MPSK Demonstration VI⁹. In this example $M = 16$, so the signal constellation displays the 16 permitted values of the complex envelope (upper left graph in Fig. 9). Fig. 10 displays the constellation in the presence of added noise, a feature which the students have incorporated into the VI. In this simulation, $M = 8$.

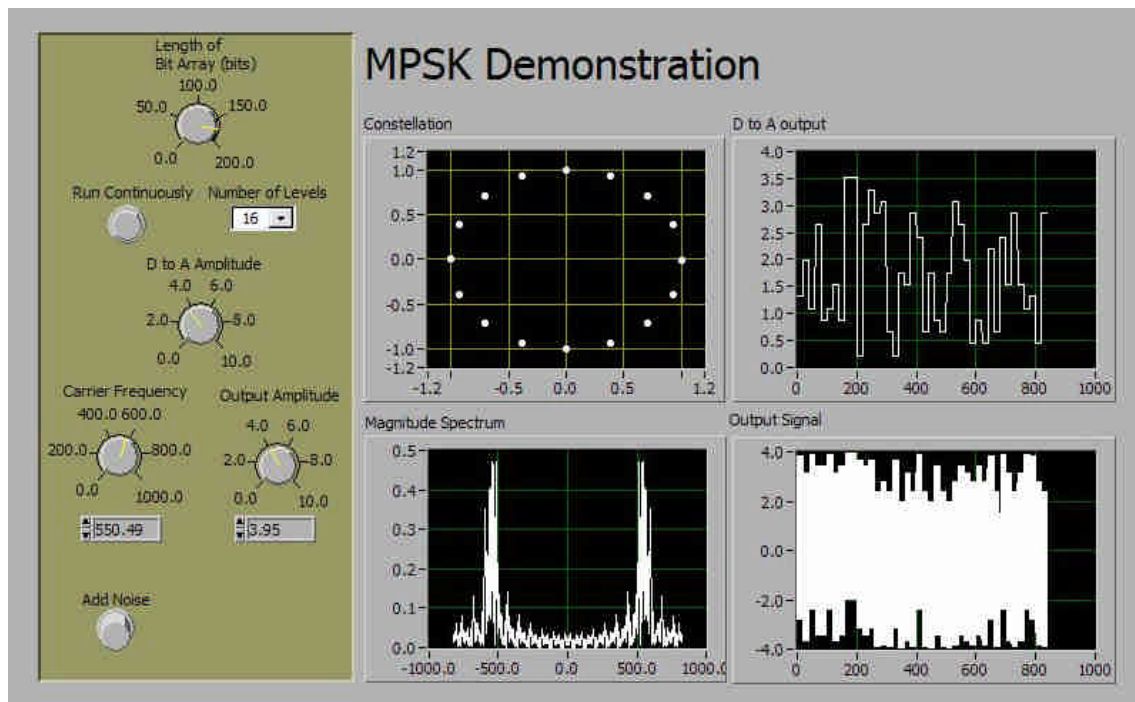


Figure 9: The front panel of the MPSK Demonstration VI.

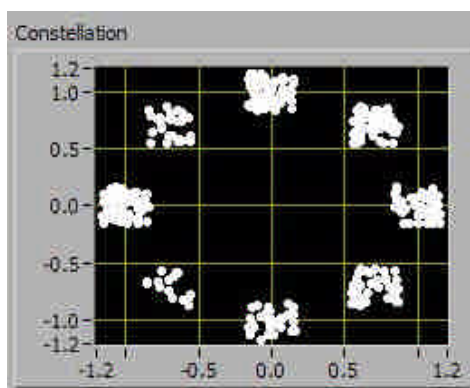


Figure 10: The signal constellation with additive noise. In this simulation $M = 8$.

V. Discussion

In this paper, I have given an account of how a virtual toolkit, the preparation of which was documented in¹, was used for the first time in my communication systems class. Section II gave an example of how a virtual instrument can enhance the presentation in class. Section III demonstrated how the availability of simulated signals and other tools can turn one demo into an exploration and prepare the ground for interesting further discussion. Section IV reported on student work along the same lines with one example.

The utilization of the tools in this toolkit is understood better with a rudimentary understanding of discrete signals. Since these are computer simulations, one would need to remember that simulations of analog processes are valid when the results of the processes all fall within the Nyquist rate determined by the original chosen sampling frequency. The discussion development in section III gave an example of a process that would result in frequencies beyond the Nyquist rate. The concept of sampling frequency gets interesting and potentially confusing when we simulate the sampling of analog signals where we can talk about two sampling frequencies: the sampling frequency of the entire simulation and the sampling frequency at which we retain samples from the simulated signal. I refer to the former as 'simulation clock frequency' and the latter as simply sampling frequency. Since my students take communication systems after DSP, I have chosen to make the simulation clock frequency as one of the inputs and expect the students to pay attention to the Nyquist rate as they implement these simulations and watch for aliasing in their simulations.

Clearly, the list of VIs in the toolkit may be expanded. Spring 2002 offering of EGR 363 has added a few and the work will be continued. There is also the task of documentation to be finished, which always seems to lag in amateur programming projects.

Students also appreciate the exposure to LabVIEW. I have noted that most senior design projects of 2002 have incorporated LabVIEW in one way or another this year. As a matter of fact, one of the senior design project teams has combined LabVIEW and MATLAB, using the LabVIEW interface to call MATLAB scripts because the LabVIEW interface is aesthetically more pleasing. As I have noted elsewhere⁷: "Part of the enthusiasm is due to the aesthetics of LabVIEW virtual instruments. I have seen many a student revisiting and perfecting the way the front panel looks long after his/her VI has achieved its computational goals and long after the class period has ended."

ACKNOWLEDGEMENTS: The LabVIEW software used in this course was purchased through a grant from Johnson Controls in Holland, MI. I would like to thank Johnson Controls for the upgrade of the electronics lab which also benefited the course mentioned in this paper. I would also like to thank Kathrine Nguru, who programmed some of the subVIs used in the VIs depicted in this paper as well as Howard Gorter and Brian Matherly, whose project is mentioned in this paper.

Bibliography

1. M. Tanyel, K. Nguru, "Preparation of a Virtual Toolkit for Communication Systems", *2002 ASEE Annual Conference and Exposition Proceedings*, Montréal, QC, June 16-19 2002.
2. Proakis, J. G., Salehi, M., *Contemporary Communication Systems using MATLAB*, Pacific Grove, CA: Brooks/Cole (2000).
3. Frederick, D., Chow, J., *Feedback Control Systems using MATLAB and the Control Systems Toolbox*, Pacific Grove, CA: Brooks/Cole (2000).
4. Ingle, V. K., Proakis, J. G., *Digital Signal Processing using MATLAB*, Pacific Grove, CA: Brooks/Cole (2000).
5. Viss, M. and Tanyel, M. "From Block Diagrams to Graphical Programs in DSP," *2001 ASEE Annual Conference & Exposition Proceedings*, Albuquerque, NM, June 24-27 2001.
6. Tanyel, M., "Enhancing the DSP Toolkit of LabVIEW", *2002 ASEE Annual Conference and Exposition Proceedings*, Montréal, QC, June 16-19 2002.
7. Tanyel, M., Adams, C., "On the Aesthetics of Computer Aided Tools for Signal Processing", *Proceedings of 64th Annual ASEE North Midwest Section Meeting*, Madison, WI, Oct. 2002.
8. Couch II, L. W., *Digital and Analog Communication Systems, Sixth Edition*, Upper Saddle River, NJ: Prentice Hall (2001).
9. Gorter, H., Matherly, B., *MPSK Demo Project Report*, EGR 363 Project Report, Dordt College, Sioux Center, IA, May 2002.

MURAT TANYEL

Murat Tanyel is a professor of engineering at Dordt College. He teaches upper level electrical engineering courses. Prior to teaching at Dordt College, Dr. Tanyel taught at Drexel University where he worked for the *Enhanced Educational Experience for Engineering Students (E⁴)* project, setting up and teaching laboratory and hands-on computer experiments for engineering freshmen and sophomores. For one semester, he was also a visiting professor at the United Arab Emirates University in Al-Ain, UAE where he helped set up an innovative introductory engineering curriculum. Dr. Tanyel received his B. S. degree in electrical engineering from Boğaziçi University, Istanbul, Turkey in 1981, his M. S. degree in electrical engineering from Bucknell University, Lewisburg, PA in 1985 and his Ph. D. in biomedical engineering from Drexel University, Philadelphia, PA in 1990.